Desalination and Water Treatment
www.deswater.com

doi: 10.1080/19443994.2013.768407

51 (2013) 5138–5148
July

Taylor & Francis
Taylor & Francis Group

Synthesis and gas transport properties of UV-cured low-viscosity fluorine-containing telechelic polyimide membranes

Ryohei Shindo, Akira Yokouchi, Hayato Shirokura, Kazuhito Yoshida, Sou Miyata, Shuichi Sato, Shinji Kanehashi, Kazukiyo Nagai*

Department of Applied Chemistry, Meiji University, 1-1-1 Higashimita, Tama-ku, Kawasaki 214-8571, Japan
Tel. +81 44 934 7211; Fax: +81 44 934 7906; email: nagai@meiji.ac.jp

Received 8 June 2012; Accepted 28 September 2012

ABSTRACT

A novel ultraviolet (UV) cross-linking method using fluorine-containing telechelic polyimide membranes was investigated. The base fluorine-containing polyimide was synthesized by polycondensation using the monomers, 4,4′-(hexafluoroisopropylidene) diphthalic anhydride (6FDA) and 2,3,5,6-tetramethyl-1,4-phenylene diamine (TeMPD). Both chain ends of the 6FDA-TeMPD polyimide were end-capped with either UV-reacted groups, 1,1-bis(acryloyl-oxy methyl) ethyl isocyanate (BEI) group or *p*-aminostyrene (PAS) group. The two types of telechelic polyimide membranes, 6FDA-TeMPD-BEI and 6FDA-TeMPD-PAS, were formed with UV irradiation from the low-viscosity solutions using the solvent-casting method. The base polyimide membrane was soluble in tetrahydrofuran, whereas both UV-cured telechelic polyimide membranes were partly insoluble in it. This result suggested that both telechelic polyimides reacted at the polymer chain ends through UV irradiation. The density values of the UV-cured membranes were almost the same. Thus, this cross-linking method could prevent significant membrane densification compared with other conventional cross-linking methods. As the UV irradiation time increased, the gas selectivity in both UV-cured polyimide membranes increased without a significant decrease in gas permeability. The increase in ideal gas selectivity was attributed to the increase in the gas diffusivity selectivity rather than the solubility selectivity.

Keywords: Polyimide; UV; Low-viscosity; Cross-linked; Gas separation; CO_2; Membrane

1. Introduction

Aromatic polyimides have been widely used as structural, electronic, and optical materials because of their good thermostability, mechanical strength, and optical properties [1–4]. Polyimides are also employed as a potting material and an interlayer dielectric membrane, because they are thermoset polymers. Among the exsisting fluorine-based polyimide membranes, fluorine-containing polyimides composed of 4,4′-(hexafluoroisopropylidene) diphthalic anhydride (6FDA) possess good gas transport and CO_2 separation properties [5–8].

In these applications, polyimide materials are generally used in membrane state. Therefore, membrane

*Corresponding author.

7th Aseanian Membrane Society Conference (AMS7), 4–7 July 2012, Busan, Korea

processability (e.g. membrane formation ability) is one of the desirable properties of industrial polyimides. Although many highly permeable gas separation membranes are available, the fabrication of asymmetric hollow fiber membranes and/or composite membranes is difficult in some cases because of their high viscosity.

The solvent-casting method is one of the useful ways of preparing porous composite membranes. However, the high viscosity of the polyimide solution causes damage to the separation layer and difficulty to form a thin layer. Hence, the use of a large quantity of casting solvents to decrease the viscosity of a polymer solution becomes an environmental burden and leads to an increase in the treatment equipment cost. Therefore, the preparation of composite membranes using a low-viscosity polymer is one of the effective approaches.

Recently, several membranes have been modified to improve gas permeability and selectivity. Cross-linking of polymer segments is one of the methods for improving gas separation performance. In addition, many cross-linking reactions for gas separation membranes were reported [9–14]. However, a trade-off relationship exists between the degree of cross-linking and gas permeability. The excessive cross-linking density of polymer membranes improves gas selectivity but significantly reduces gas permeability because of membrane densification [10,11,15–18].

This study hypothesizes that one of the effective cross-linking approaches is crosslinked at the polymer chain ends using telechelic polymers. A small degree of cross-linking structure could prevent membrane densification and decrease in gas permeability. In addition, CO_2-induced membrane plasticization, which is a serious problem on gas separation application, could also be improved because the polymer chain ends have the high mobility in the polymer chain and related to the membrane plasticization through this cross-linking method.

In this study, the highly gas permeable 6FDA-2,3,5,6-tetramethyl-1,4-phenylene diamine (TeMPD) polyimide was used as a base polymer. We synthesized two types of novel low-viscosity telechelic polyimide containing either 1,1-bis(acryloyloxy methyl ethyl isocyanate (BEI) or *p*-aminostyrene (PAS) in both chain ends of the 6FDA-TeMPD polymer. The physical, thermal, and gas permeation properties of ultraviolet (UV)-cured polyimide membranes were investigated.

2. Experimental

2.1. Materials

The monomers used in the synthesis, including 6FDA, *p*-aminophenethyl alcohol (APA), PAS (Sigma-Aldrich Co.), TeMPD (Tokyo Chemical Industry Co., Ltd), and BEI (Showa Denko K. K.), were used as-received without further purification. *N*-methyl-2-pyroridone (NMP, Junsei Chemical. Co., Ltd), a polymerization solvent; *p*-xylene (Junsei Chemical. Co., Ltd), an azeotropic agent; tetrahydrofuran (THF, Junsei Chemical. Co., Ltd); and *N*,*N*-dimethylacetamide (DMAc, Junsei Chemical. Co., Ltd) were dehydrated with well-dried 4A molecular sieves. Pyridine and acetic anhydride (Junsei Chemical. Co., Ltd) were used as chemical imidization catalysts. Dibutyltin dilaurate (DBTDL, Tokyo Chemical Industry Co., Ltd) was also used as a catalyst. 1-Hydroxy cyclohexylphenyl ketone (Irg184, Japan Chibagaigi Co., Ltd), a photopolymerization initiator, was used as-received without further purification.

2.2. Syntheses of polyimides

2.2.1. 6FDA-TeMPD-BEI

The synthesis of the base polyimide 6FDA-TeMPD was based on the literature [7]. Scheme 1(a) shows the synthesis of 6FDA-TeMPD-BEI ([6FDA]/[TeMPD]/[BEI] = 100/90/20 M ratio). N_2 purge was performed for 30 min to replace H_2O in the four-necked separable flask. Subsequently, TeMPD (1.66 g, 10.1 mmol) and APA (0.309 g, 2.25 mmol) were dissolved in 11.2 g NMP with constant stirring for 30 min. Subsequently, 6FDA (5.00 g, 11.3 mmol) was added into the solution and dissolved in 16.7 g NMP with constant stirring for 6 h. NMP (6.15 g) and *p*-xylene (4.78 g) were added with constant stirring for 4 h at 180˚C. Then, BEI (1.62 g, 6.75 mmol) and DBTDL as activated catalysts were added to the flask slowly with constant stirring for 13 h at 60˚C. An equimolar APA amount of BEI (0.539 g, 2.25 mmol) was again added, and the solution was stirred for 4 h. This low-viscosity brown solution was poured into methanol. The product of 6FDA-TeMPD-BEI was purified using the solution-reprecipitation purification process by the THF–methanol solvent and then dried for 24–48 h under vacuum at 40˚C.

2.2.2. 6FDA-TeMPD-PAS

Scheme 1(b) shows the synthesis of 6FDA-TeMPD-PAS ([6FDA]/[TeMPD]/[PAS] = 100/90/20 M ratio). N_2 purge was performed for 30 min to replace H_2O in the four-necked separable flask. Then, TeMPD (1.66 g, 10.1 mmol) and PAS (0.268 g, 2.25 mmol) were dissolved in 10.9 g NMP with constant stirring for 30 min. Subsequently, 6FDA (5.00 g, 11.3 mmol) was added into the solution and dissolved in 16.8 g NMP with constant stirring for 6 h. Next, the imidization

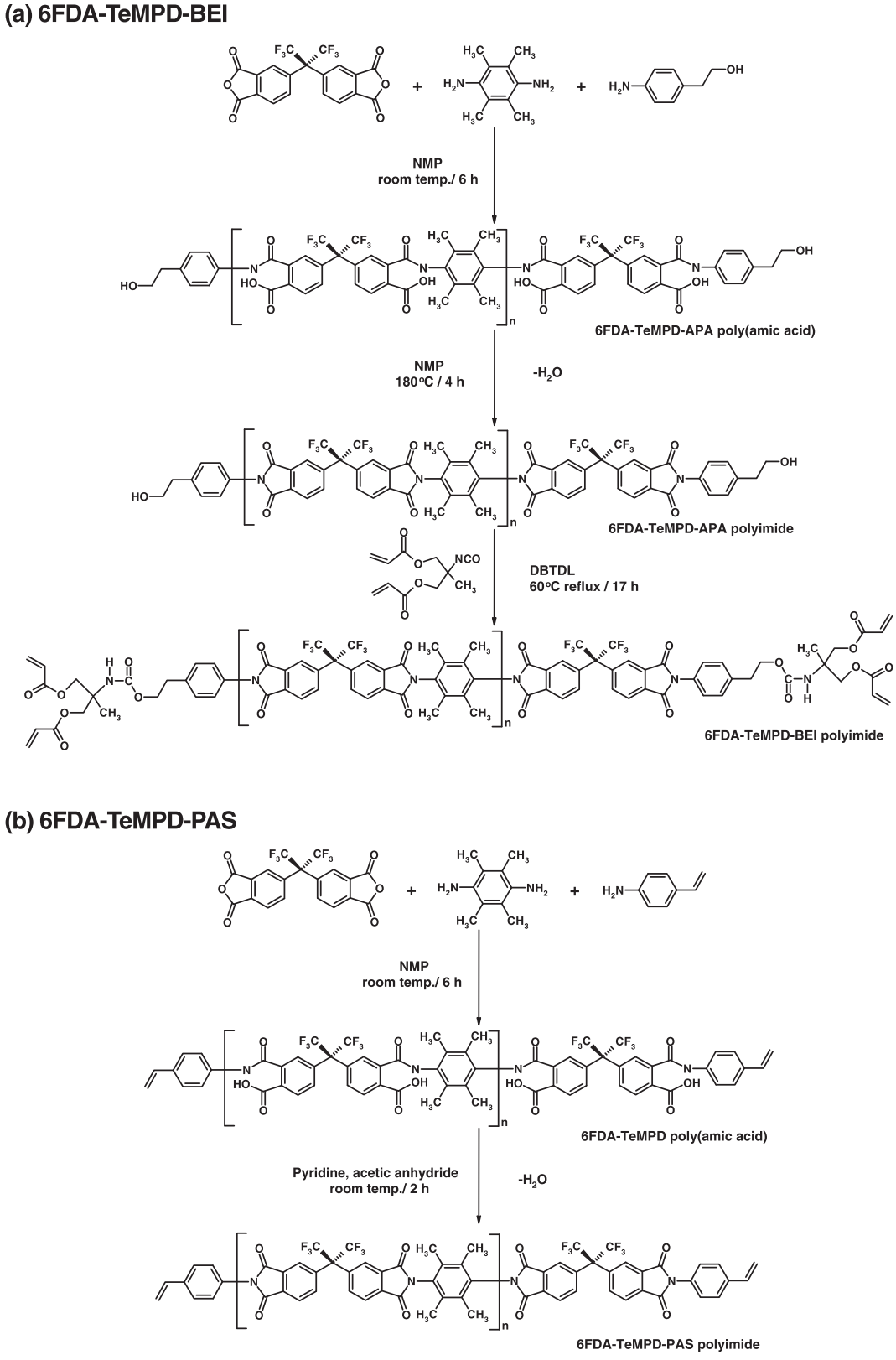

Scheme 1. Synthesis of the (a) 6FDA-TeMPD-BEI and (b) 6FDA-TeMPD-PAS.

process was performed at room temperature using chemical imidization catalysts. The catalysts pyrridine (6.23 g) and acetic anhydride (5.75 g) were added along with NMP (11.6 g) with constant stirring for 2 h. This low-viscosity brown solution was poured into methanol. The product of 6FDA-TeMPD-PAS was purified using the solution-reprecipitation purification process by the THF–methanol solvent and then dried for 24–48 h under vacuum at 40°C.

2.3. Membrane preparation

All membranes were prepared through the solvent-casting method. 6FDA-TeMPD-BEI membranes were prepared by casting a filtered 11–12 wt.% polymer solution in DMAc onto a Petri dish. 6FDA-TeMPD and 6FDA-TeMPD-PAS membranes were prepared by casting a filtered 3 wt.% polymer solution in THF onto a Petri dish. UV irradiation was carried out using a high-pressure mercury lamp (100 W, Riko-Kagaku Sangyo Co. Ltd.,) under nitrogen atmosphere at the distance of 15 cm with 3–4 wt.% Irg184. In this study, UV irradiation was conducted for 0, 30, 120, and 360 min. After UV irradiation, the 6FDA-TeMPD-BEI cast solution was left at 35°C under vacuum for 24–48 h to volatilize the solvent. Then, the obtained membranes were dried at 150°C under vacuum for 48 h to eliminate any residual solvent. The 6FDA-TeMPD-PAS cast solution was also left at 35°C under vacuum for 24–48 h to volatilize the solvent. The thickness of the membranes used in this study varied from 80 to 120 μm.

2.4. Structure analysis and characterization

All characterization data were determined in the membrane state for at least three samples to confirm the reproducibility of the experimental results.

^{1}H NMR and ^{13}C NMR were performed at 25°C with JNM-ECA500 (JEOL Ltd., Tokyo, Japan). Chloroform-*d* (ISOTEC Inc.) was used as a solvent.

Fourier transform-infrared spectrometry (FT-IR) was carried out using the KBr method with FT/IR-4100 (JASCO Co., Tokyo, Japan). The measurement conditions were as follows: resolution, 2 cm^{-1}; multiplication number, 32 times; and temperature, 23 ± 1°C.

The weight average molecular weight, M_w, the number average molecular weight, M_n, and the molecular weight distribution ratio, M_w/M_n, of the polymer were determined using a gel permeation chromatograph (GPC; HLC-8220, Tosoh Co., Tokyo, Japan) with TSK-gel columns (SuperAWM-H) and a detector (RI-8220). The calibration was performed by polystyrene standards at 40°C in a THF solvent at a flow rate of 0.300 mL/min. Inherent viscosity (η) of polymers was measured using a Canon Fensuke viscometer (YOSHIDA SEISAKUSHO Co., Ltd). Sample solution was dissolved in 0.2, 0.3, 0.4, and 0.5 g/dL *N*,*N*-dimethylform amide (DMF, Junsei Chemical. Co., Ltd) solution. The fall time of the predetermined quantity of sample solutions was measured at 30°C.

Gel fraction measurement of the UV-cured membranes was conducted by extracting the membranes in THF for 24 h. The measurement temperature was set to 23 ± 1°C. The insoluble fractions were vacuum dried at 35°C for approximately 24 h.

Membrane density (ρ) was determined by flotation of the small membrane samples in a density gradient column, which was maintained at 23 ± 1°C.

Wide-angle X-ray diffraction (WAXD) measurements were performed on a Rint1200 X-ray diffractometer (Rigaku, Co., Ltd, Tokyo, Japan) using a Cu-Kα radiation source. The wavelength of the radiation was 1.54 Å, and 2θ was the maximum intensity in a halo peak. The *d*-spacing was estimated from Bragg's equation using the maximum intensity in an amorphous scattering halo peak.

Thermogravimetric analysis (TGA) was carried out using a Pyris 1 TGA Thermo Gravimetric Analyzer (PerkinElmer, Inc., Shelton, USA). The polymer sample of ca. 1.0 mg was heated from 50 to 700°C in a platinum pan at a heating rate of 10°C/min under nitrogen atmosphere at a flow rate of 60 mL/min.

2.5. Gas permeation properties

The permeability coefficient (*P*) of pure gases [i.e. hydrogen (H_2), oxygen (O_2), nitrogen (N_2), carbon dioxide (CO_2), and methane (CH_4)] in polyimide membranes was determined at 35 ± 1°C using the constant-volume/variable-pressure method, according to the literature [19,20]. The feed pressure was between 75 and 77 cmHg, and the permeate side was maintained under vacuum. All permeation data were determined for at least three samples to ensure the reproducibility of the experimental results.

The apparent diffusion coefficient (*D*) was determined from membrane thickness (ℓ) and time lag (θ), the period of time needed to reach the steady state:

$$D = \frac{\ell^2}{6\theta} \tag{1}$$

According to the solution-diffusion mechanism, the apparent solubility coefficient (*S*) can be evaluated as follows:

$$S = \frac{P}{D} \tag{2}$$

The ideal gas selectivity (α) of Gas A over B was expressed as the ratio of the permeability coefficient of Gas A over that of Gas B.

$$\alpha_{A/B} = \frac{P_A}{P_B} \tag{3}$$

3. Results and discussion

3.1. Polymer structure and characterization

The polyimides were characterized according to their chemical structure, as presented in Scheme by ^{1}H NMR and ^{13}C NMR and FT-IR analyses.

6FDA-TeMPD-BEI ^{1}H NMR (500 MHz, $CDCl_3$, δ): 7.99 (2H, H^1), 8.10 (2H, H^2), 7.96 (2H, H^3), 2.11 (12H, H^4), 7.39 (4H,H^5), 3.00 (2H,H^6), 4.38 (2H,H^7), 5.03 (1H, H^8), 1.41 (3H,H^9), 4.30 (4H,H^{10}), 6.11 (2H,H^{11}), 6.40 (2H,H^{12}), 5.85 (2H,H^{13}). ^{13}C NMR (500 MHz, $CDCl_3$, δ): 165.98 (C^1), 165.75 (C^2), 132.77 (C^3), 132.42 (C^4), 125.47 (C^5), 124.27 (C^6), 139.21 (C^7), 136.02 (C^8), 65.27 (C^9), 122.27 (C^{10}), 130.82 (C^{11}), 134.01 (C^{12}), 15.68 (C^{13}), 124.53 (C^{14}), 129.74 (C^{15}), 126.53 (C^{16}), 119.96 (C^{17}), 35.03 (C^{18}), 65.51 (C^{19}), 166.19 (C^{20}), 54.90 (C^{21}), 65.96 (C^{22}), 165.67 (C^{23}), 127.76 (C^{24}), 131.58 (C^{25}), 19.40 ppm (C^{26}). FT-IR (KBr, cm^{-1}): 1,786 (C=O asymmetric stretching), 1,725 (C=O symmetric stretching), 1,355 (C–N stretching), 724 (C=O bending).

6FDA-TeMPD-PAS ^{1}H NMR (500 MHz, $CDCl_3$, δ): 7.99 (2H, H^1), 8.10 (2H, H^2), 7.96 (2H, H^3), 2.13 (12H, H^4), 7.40 (2H, H^5), 7.56 (2H, H^6), 6.77 (1H, H^7), 5.33 (1H, H^8), 5.80 (1H, H^9). ^{13}C NMR (500 MHz, $CDCl_3$, δ): 166.05 (C^1), 165.81 (C^2), 132.82 (C^3), 132.48 (C^4), 125.56 (C^5), 124.34 (C^6), 139.28 (C^7), 136.05 (C^8), 65.14 (C^9), 122.30 (C^{10}), 130.88 (C^{11}), 134.06 (C^{12}), 15.78 (C^{13}), 124.61 (C^{14}), 127.00 (C^{15}), 126.56 (C^{16}), 135.85 (C^{17}), 137.90 (C^{18}), 115.38 (C^{19}). FT-IR (KBr, cm^{-1}): 1,786 (C=O asymmetric stretching), 1,725 (C=O symmetric stretching), 1,355 (C–N stretching), 724 (C=O bending) (Fig. 1).

Table 1 presents the summary of the physical properties of the synthesized telechelic polyimides. The GPC elution curve of each polyimide sample showed a single broad peak. The M_n, M_w and M_w/M_n of 6FDA-TeMPD were estimated to be 100,000, 160,000 g/mol, and 1.6, respectively; those of 6FDA-TeMPD-BEI were 10,000, 14,000 g/mol, and 1.4, respectively; and those of 6FDA-TeMPD-PAS were 12,000, 19,000 g/mol, and 1.6, respectively. The molecular weight of both polyimides could be controlled using the mono-amine component and the feed ratio. The M_n values of both telechelic polyimides determined using ^{1}H NMR were approximately 9,000 and 8,000 g/mol. The molecular weight determined from GPC measurement was similar to that determined from ^{1}H NMR. This result suggests that both telechelic polyimides were able to introduce the UV-reacted functional groups at the polymer chain ends.

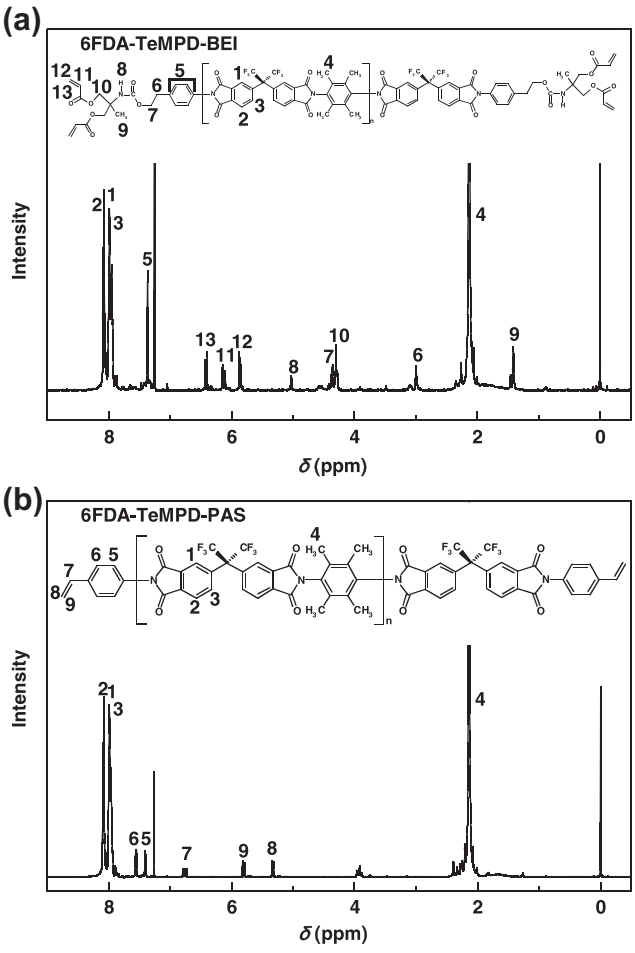

Fig. 1. ^{1}H NMR spectra of the (a) 6FDA-TeMPD-BEI and (b) 6FDA-TeMPD-PAS.

The inherent viscosity of both terechelic polyimides was 0.19 dL/g, which was 74% smaller compared with that of 6FDA-TeMPD (0.74 dL/g).

Fig. 2 shows the photographs of the polyimide membranes. As base polyimide, 6FDA-TeMPD formed a self-standing light-yellow transparent membrane. By contrast, both UV-uncured polyimide membranes were very brittle because of the weak entanglement of polymers. These molecular weights were controlled at approximately 10,000 g/mol to obtain low viscosity. Therefore, the solid properties of the UV-uncured membranes could not be measured. On the other hand, both UV-cured membranes were good self-standing light-yellow membranes with increasing UV irradiation time. This result suggests that the cross-linking reaction could occur at the polymer chain ends.

Table 1
Characterization of the 6FDA-TeMPD-BEI and 6FDA-TeMPD-PAS

Polymer	M_n[a] (g/mol)	M_w[a] (g/mol)	M_w/M_n[a]	M_n[b] (g/mol)	η (dL/g)
6FDA-TeMPD	100,000	160,000	1.6	–	0.74
6FDA-TeMPD-BEI	10,000	14,000	1.4	9,000	0.19
6FDA-TeMPD-PAS	12,000	19,000	1.6	8,000	0.19

[a]Determined by GPC measurement using polystyrene standard in THF.
[b]Determined by ^{1}H NMR measurement.

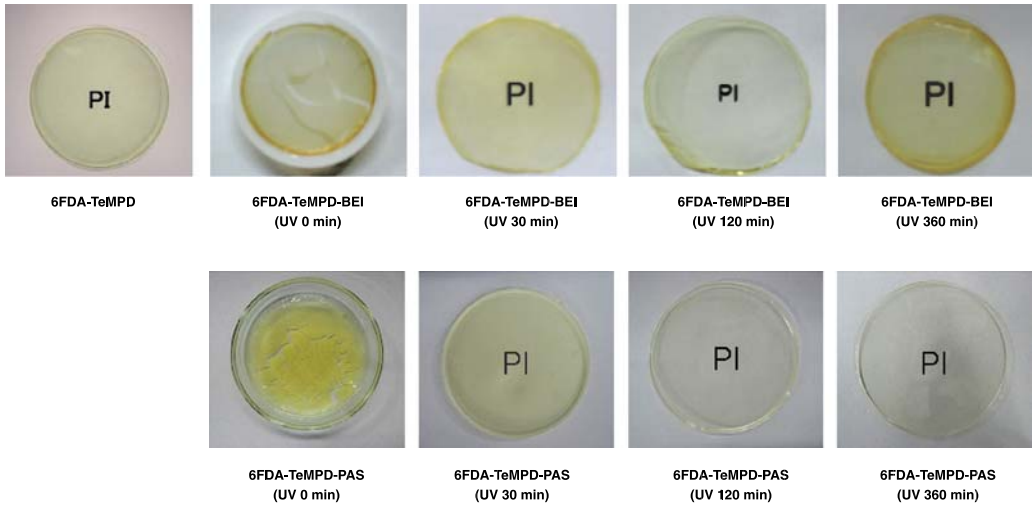

Fig. 2. Photographs of the UV-cured 6FDA-TeMPD-BEI and 6FDA-TeMPD-PAS membranes.

Fig. 3 shows the FT-IR spectra of these polyimide membranes. The specific peaks, 1,730 cm^{-1} (C=O stretching) and 1,350 cm^{-1} (C–N stretching), which are the characteristic bands of polyimide, were observed in all polyimide membranes. This finding suggests that chemical structure changes did not occur in the 6FDA-TeMPD polyimide. In addition, each UV-cured membrane increased alkane peak at 2,950 cm^{-1}, which was attributed to the cross-linking reaction at the polymer chain ends with increasing UV irradiation time. Therefore, the double bond at the polymer chain ends (i.e. acryloyl or vinyl group) reacted by UV irradiation and formed a crosslinked structure.

Table 2 summarizes the physical properties of the polyimide membranes. The base 6FDA-TeMPD and both UV-uncured telechelic polyimide membranes were soluble in THF, chloroform, and amine solvents such as DMAc, DMF, and NMP, whereas both UV-cured telechelic polyimide membranes were partly insoluble in the solvents. This result suggests that both telechelic polyimides reacted at the polymer chain ends through UV irradiation. Fig. 4 shows the relationship between the gel fraction of UV-cured membranes and UV irradiation time. The insoluble gel component was obtained after UV irradiation, presenting the crosslinked UV-cured membranes. The gel fraction increased with increasing UV irradiation time with each UV-cured membrane, and it became constant in approximately 60% for 6FDA-TeMPD-BEI and in approximately 80% for 6FDA-TeMPD-PAS at over 120 min of UV irradiation. These results suggest that the cross-linking reaction at the polymer chain ends was almost completed at over 120 min. In the conventional UV cross-linking method, BTDA-containing polyimides have almost 100% of gel fraction after UV irradiation [11]. Based on these results, our novel cross-linking approach using telechelic polyimides could prevent excess membrane densification. Furthermore, the terminal group content in the UV-cured membranes determined by ^{1}H NMR decreased with increasing UV irradiation time, suggesting that the UV cross-linking reaction could occur at the polymer chain ends. The density of 6FDA-TeMPD was 1.34 g/cm^3, whereas that of the UV-cured membranes was from 1.34 to 1.35 g/cm^3 for 6FDA-TeMPD-BEI, and 1.32 to 1.36 g/cm^3 for 6FDA-TeMPD-PAS, respectively. Although the cross-linking reaction proceeded and increased the gel fraction of the UV-cured

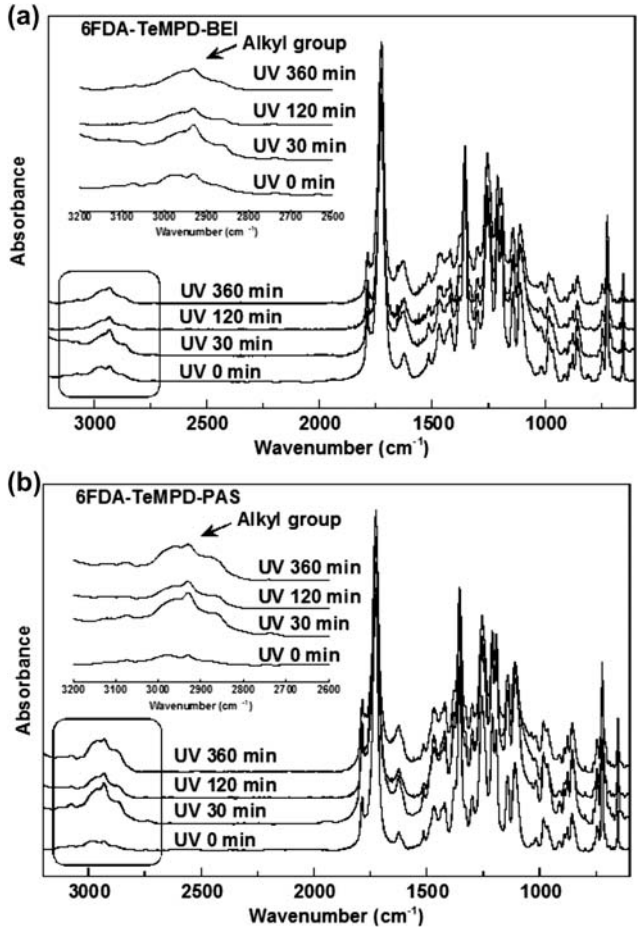

Fig. 3. FT-IR spectra of the UV-cured (a) 6FDA-TeMPD-BEI and (b) 6FDA-TeMPD-PAS membranes.

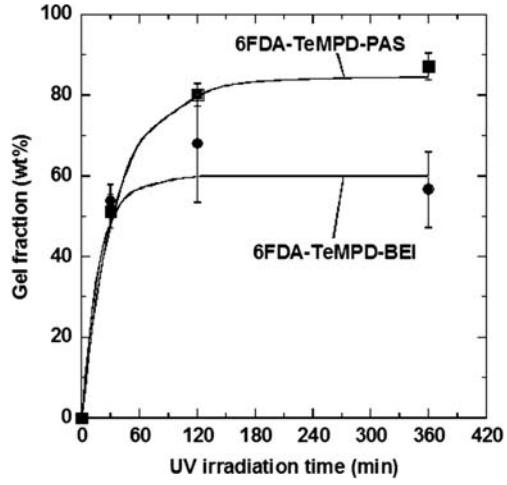

Fig. 4. UV irradiation time dependence on the gel fraction of the UV-cured 6FDA-TeMPD-BEI and 6FDA-TeMPD-PAS membranes.

polyimide membranes, this method could prevent membrane densification.

Fig. 5 shows the WAXD patterns of these polyimide membranes. All polyimide membranes were completely amorphous because a single broad halo was observed in all membranes. The *d*-spacing value of 6FDA–TeMPD calculated using Bragg's condition was 6.2 ± 0.1 Å, whereas that of the UV-cured membranes was almost the same (from 5.8 to 5.9 Å), which were below 5–9% smaller than the base polymer. As expected from the density measurement, the cross-linking reaction at the polymer chain ends suppressed the increase in the degree of cross-link density.

Fig. 6 shows the TGA curves for the polyimide membranes. In all polyimide membranes, the thermal degradation was observed from 550°C, which was attributed to the decomposition of the 6FDA-TeMPD polyimide backbone. Hence, the thermal stability of the main 6FDA-TeMPD polyimide component did not affect the cross-linking reaction at the polymer chain ends. 6FDA-TeMPD and UV-uncured 6FDA-TeMPD-PAS membranes showed one-step decomposition, whereas UV-uncured 6FDA-TeMPD-BEI and both

Table 2
Physical properties of the UV-cured 6FDA-TeMPD-BEI and 6FDA-TeMPD-PAS membranes

Polymer	UV irradiation time (min)	Gel fraction (wt.%)	Terminal group content[a] (mol%)	ρ (g/cm^3)	*d*-spacing (Å)
6FDA-TeMPD	0	0.0	–	1.342 ± 0.003	6.2 ± 0.1
6FDA-TeMPD-BEI	0	0.0	6.52 ± 0.48	N/A	N/A
	30	53.8 ± 4.1	4.62 ± 1.35	1.344 ± 0.001	5.8 ± 0.1
	120	68.1 ± 14.6	3.28 ± 0.06	1.345 ± 0.001	5.8 ± 0.1
	360	56.6 ± 9.4	0.00	1.350 ± 0.001	5.3 ± 0.1
6FDA-TeMPD-PAS	0	0.0	7.20 ± 0.03	N/A	N/A
	30	51.2 ± 4.1	3.98 ± 0.80	1.323 ± 0.001	5.9 ± 0.1
	120	80.2 ± 2.9	0.00	1.332 ± 0.001	5.8 ± 0.1
	360	87.2 ± 3.3	0.00	1.367 ± 0.002	5.8 ± 0.1

[a]Determined by ^{1}H NMR measurement.

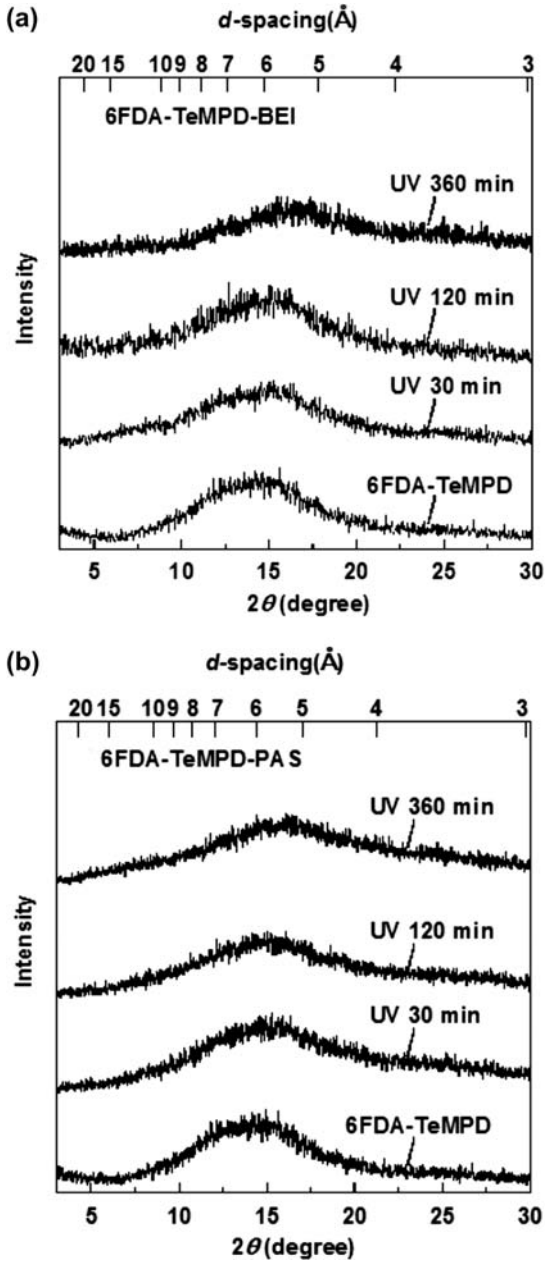

Fig. 5. Wide angle X-ray diffraction patterns of the UV-cured (a) 6FDA-TeMPD-BEI and (b) 6FDA-TeMPD-PAS membranes.

UV-cured membranes showed multiple-step decomposition behavior. This multiple-step decomposition could be attributed to the alkyl structure in the 6FDA-TeMPD-BEI polyimide. As the UV irradiation time increased, that is, the cross-linking reaction proceeded, the weight of the first thermal decomposition tended to increase. This finding suggests that the styrene structure formed by the cross-linking reaction in the acryloyl or vinyl groups thermally decomposed.

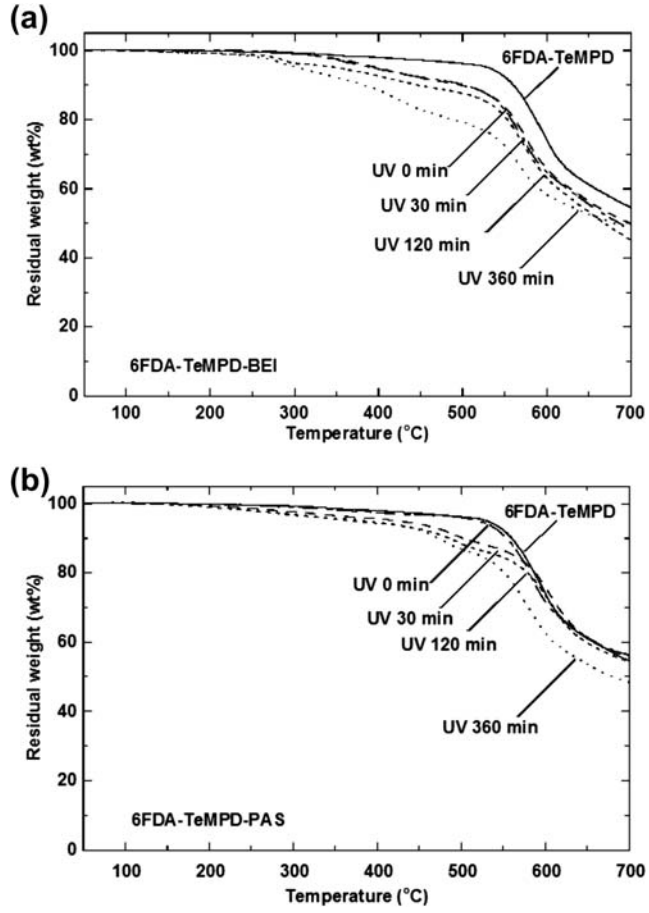

Fig. 6. TGA curves of the UV-cured (a) 6FDA-TeMPD-BEI and (b) 6FDA-TeMPD-PAS membranes.

3.2. Gas permeation properties

Gas permeability measurement conducted except for the UV-uncured membrane and UV-cured 360 min of 6FDA-TeMPD-BEI, because these membranes were brittle and caused cracking. In this study, any hysteresis in the permeation data in all membranes was not observed. Only, the maximum prediction value of each coefficient was estimated for comparison because the time lag of hydrogen was shorter, making a highly accurate detection difficult.

Table 3 summarizes the gas permeability coefficient of the polyimide membranes. The CO_2 permeability coefficient of the base 6FDA-TeMPD polyimide membrane was 4.28×10^{-8} cm^3 (STP)cm/(cm^2 s cmHg), whereas that of UV-cured 6FDA-TeMPD-BEI decreased by approximately 70% compared with 6FDA-TeMPD. By contrast, the gas permeability coefficient of UV-cured 6FDA-TeMPD-PAS decreased from approximately 20% to 70%. As expected to the density of the UV-cured membranes, the gas permeability of the

Table 3
Gas permeability coefficient of the UV-cured 6FDA-TeMPD-BEI and 6FDA-TeMPD-PAS membranes

Polymer	UV irradiation time (min)	Permeability coefficient ($\times 10^{-10}$ cm^3(STP)cm/(cm^2 s cmHg))				
		H_2	O_2	N_2	CO_2	CH_4
6FDA-TeMPD	0	336 ± 2	71.2 ± 1.5	19.7 ± 0.1	428 ± 2	17.2 ± 0.1
6FDA-TeMPD-BEI	0	N/A	N/A	N/A	N/A	N/A
	30	115 ± 2	19.5 ± 0.1	4.93 ± 0.10	120 ± 1	4.42 ± 0.06
	120	161 ± 2	24.8 ± 0.3	5.87 ± 0.12	138 ± 1	4.53 ± 0.03
	360	N/A	N/A	N/A	N/A	N/A
6FDA-TeMPD-PAS	0	N/A	N/A	N/A	N/A	N/A
	30	291 ± 6	44.5 ± 0.9	10.3 ± 0.2	272 ± 6	10.1 ± 0.2
	120	317 ± 21	54.1 ± 3.6	13.8 ± 0.9	338 ± 23	12.5 ± 0.8
	360	158 ± 9	19.8 ± 1.1	4.58 ± 0.26	128 ± 7	3.88 ± 0.22

UV-cured 6FDA-TeMPD-BEI was lower than that of the UV-cured 6FDA-TeMPD-PAS.

Table 4 summarizes the apparent gas diffusion coefficient of the polyimide membranes. The CO_2 diffusion coefficient of 6FDA-TeMPD was 1.09×10^{-7} cm^2/s, whereas that of UV-cured 6FDA-TeMPD-BEI decreased from approximately 60–70% compared with 6FDA-TeMPD. By contrast, the CO_2 diffusion coefficient of UV-cured 6FDA-TeMPD-PAS decreased from approximately 0–50%. The gas diffusivity of the UV-cured 6FDA-TeMPD-PAS membranes was higher than that of the UV-cured 6FDA-TeMPD-BEI. These results suggest that the 6FDA-TeMPD-PAS membranes greatly suppressed the densification compared with 6FDA-TeMPD-BEI, thereby preventing gas diffusivity reduction.

Table 5 summarizes the apparent gas solubility coefficient of the polyimide membranes. The CO_2 solubility coefficient of 6FDA-TeMPD was 0.392 cm^3 (STP)/(cm^3 cmHg), whereas that of UV-cured 6FDA-TeMPD-BEI decreased from approximately 10% to 30% compared with 6FDA-TeMPD. By contrast, the CO_2 solubility coefficient of UV-cured 6FDA-TeMPD-PAS gradually decreased from approximately 25% to 40% with increasing UV irradiation time. The gas permeability of the UV-cured membranes was affected by both gas diffusion coefficient and gas solubility coefficient, particularly for the gas diffusivity rather than the solubility.

Table 6 summarizes the ideal gas selectivity of the polyimide membranes. The gas selectivity of both UV-cured membranes was higher than that of 6FDA-TeMPD membrane. This increase in the ideal gas selectivity was attributed to the increase in the gas diffusivity selectivity rather than the solubility selectivity. Fig. 7 shows the relationship between $\alpha(H_2/CH_4)$ separation performance and Robeson's upper bound [21]. The UV-cured 6FDA-TeMPD-BEI and 6FDA-TeMPD-PAS membranes showed higher H_2 gas permeability as compared with other aromatic polyimide membranes. The gas selectivity $\alpha(H_2/CH_4)$ of 6FDA-TeMPD was 19.5, whereas that of 6FDA-TeMPD-BEI and

Table 4
Gas diffusion coefficient of the UV-cured 6FDA-TeMPD-BEI and 6FDA-TeMPD-PAS membranes

Polymer	UV irradiation time (min)	Diffusion coefficient ($\times 10^{-8}$ cm^2/s)				
		H_2	O_2	N_2	CO_2	CH_4
6FDA-TeMPD	0	–	33.7 ± 0.5	11.2 ± 0.2	10.9 ± 0.1	2.76 ± 0.05
6FDA-TeMPD-BEI	0	–	N/A	N/A	N/A	N/A
	30	–	14.2 ± 0.7	4.98 ± 0.53	4.73 ± 0.03	1.19 ± 0.03
	120	–	13.1 ± 0.2	3.74 ± 0.12	3.87 ± 0.10	0.801 ± 0.026
	360	–	N/A	N/A	N/A	N/A
6FDA-TeMPD-PAS	0	–	N/A	N/A	N/A	N/A
	30	–	31.4 ± 0.7	6.08 ± 0.13	9.38 ± 0.20	1.76 ± 0.04
	120	–	41.2 ± 2.8	10.4 ± 0.7	11.9 ± 0.8	2.47 ± 0.17
	360	–	21.2 ± 1.2	5.09 ± 0.29	5.50 ± 0.31	0.939 ± 0.054

Table 5
Gas solubility of the UV-cured 6FDA-TeMPD-BEI and 6FDA-TeMPD-PAS membranes

Polymer	UV irradiation time (min)	Solubility coefficient ($\times 10^{-2}$ cm^3(STP)/(cm^3 cmHg))				
		H_2	O_2	N_2	CO_2	CH_4
6FDA-TeMPD	0	–	2.11 ± 0.03	1.77 ± 0.16	39.2 ± 0.1	6.23 ± 0.07
6FDA-TeMPD-BEI	0	–	N/A	N/A	N/A	N/A
	30	–	1.38 ± 0.07	1.00 ± 0.09	25.4 ± 0.1	3.72 ± 0.14
	120	–	1.89 ± 0.04	1.57 ± 0.08	35.7 ± 1.1	5.65 ± 0.20
	360	–	N/A	N/A	N/A	N/A
6FDA-TeMPD-PAS	0	–	N/A	N/A	N/A	N/A
	30	–	1.42 ± 0.03	1.70 ± 0.04	29.1 ± 0.6	5.75 ± 0.12
	120	–	1.31 ± 0.09	1.34 ± 0.09	28.4 ± 1.9	5.04 ± 0.34
	360	–	0.934 ± 0.053	0.901 ± 0.052	23.3 ± 1.3	4.14 ± 0.24

Table 6
Ideal gas selectivity of the UV-cured 6FDA-TeMPD-BEI and 6FDA-TeMPD-PAS membranes

Polymer	UV irradiation time (min)	Gas selectivity				
		H_2/N_2	H_2/CH_4	CO_2/N_2	CO_2/CH_4	O_2/N_2
6FDA-TeMPD	0	17.0 ± 0.2	19.5 ± 0.2	21.7 ± 0.2	24.9 ± 0.3	3.61 ± 0.09
6FDA-TeMPD-BEI	0	N/A	N/A	N/A	N/A	N/A
	30	23.3 ± 0.9	26.0 ± 0.8	24.3 ± 0.7	27.2 ± 0.6	3.95 ± 0.10
	120	27.3 ± 1.0	35.5 ± 0.7	23.6 ± 0.6	30.6 ± 0.4	4.22 ± 0.14
	360	N/A	N/A	N/A	N/A	N/A
6FDA-TeMPD-PAS	0	N/A	N/A	N/A	N/A	N/A
	30	28.2 ± 0.6	28.7 ± 0.6	26.4 ± 0.6	26.9 ± 0.6	4.32 ± 0.09
	120	22.9 ± 1.5	25.4 ± 1.7	24.4 ± 1.6	27.1 ± 1.8	3.91 ± 0.26
	360	34.6 ± 2.0	40.8 ± 2.3	27.9 ± 1.6	33.0 ± 1.9	4.33 ± 0.25

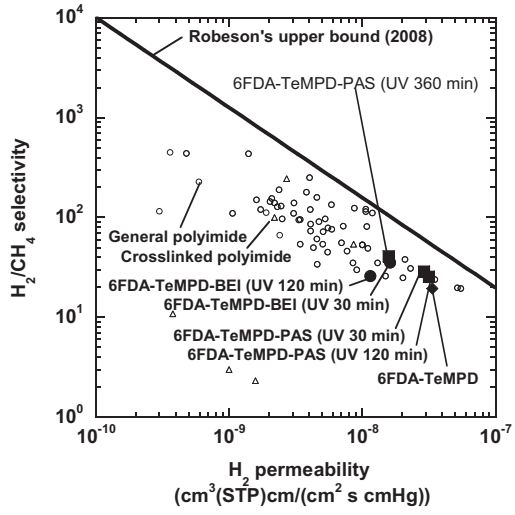

Fig. 7. Relationship between H_2 permeability and H_2/CH_4 gas selectivity for the UV-cured membranes with Robeson's upper bound [21]. The represented symbols are, 6FDA-TeMPD-BEI (●), 6FDA-TeMPD-PAS (■), 6FDA-TeMPD (◆), general polyimide (○), crosslinked polyimide (△).

6FDA-TeMPD-PAS was over 25. These results can be attributed to the increase in gas selectivity based on the differences in molecular size by the formation of the cross-linking structure at the polymer chain ends. Therefore, the cross-linking reaction of telechelic polyimides at the polymer chain ends using UV irradiation was more effective than the conventional cross-linking for the improvement of gas selectivity and the suppression of significant decrease in gas permeability.

4. Conclusion

Two types of low-viscosity fluorine-containing telechelic polyimides containing acryloyl or vinyl groups at the polymer chain ends were synthesized. Both chain ends of the 6FDA-TeMPD base polymer were end-capped with either BEI or PAS with a UV-reacted functional group. The molecular weight and inherent viscosity of both telechelic polyimides were 10,000–12,000 g/mol and 0.19 dL/g, respectively. The two types of telechelic polyimide membranes,

6FDA-TeMPD-BEI and 6FDA-TeMPD-PAS, were formed with UV irradiation from the low-viscosity solutions by the solvent-casting method. Both UV-cured membranes were good self-standing light-yellow membranes with increasing UV irradiation time. This result suggests that the UV cross-linking reaction could occur at the polymer chain ends. The gas selectivity of both UV-cured membranes increased with increasing UV irradiation time as compared with 6FDA-TeMPD polyimide. These results were attributed to an increase in gas selectivity based on the differences in molecular size by the formation of the cross-linking structure at the polymer chain ends. Therefore, the cross-linking reaction of telechelic polyimides at the polymer chain ends using UV irradiation was more effective than the conventional cross-linking for the improvement of gas selectivity and the suppression of significant decrease in gas permeability.

Acknowledgments

This research was partially supported by a Grant-in-aid for Scientific Research C (24560862) from the Ministry of Education, Culture, Sports, Science and Technology, Japan, the Japanese Society of the Promotion of Science and Research Project Grant B (3) from the Institute of Science and Technology, Meiji University, Japan.

Nomenclature

D — apparent diffusion coefficient (cm^2/s)
ℓ — membrane thickness (cm)
M_n — number average molecular weight (g/mol)
M_w — weight average molecular weight (g/mol)
P — permeability coefficient (cm^3 (STP) cm/(cm^2 s cmHg))
S — apparent solubility coefficient (cm^3 (STP)/(cm^3 cmHg))

Greek symbols

α — ideal gas selectivity
η — inherent viscosity (dL/g)
ρ — membrane density (g/cm^3)
θ — time-lag (s)

References

[1] P.M. Hergenrother, Perspectives in the development of high-temperature polymers, Angew. Chem. Int. Ed. 29 (1990) 1262–1268.
[2] T. Homma, Y. Kutsuzawa, K. Kunimune, Y. Murao, Stability of a new polyimide siloxane film as interlayer dielectrics of ULSI multilevel interconnections, Thin Solid Films 235 (1993) 80–85.
[3] W.L. Chang, H.W. Su, W.C. Chen, Synthesis and properties of photosensitive polyimide-nanocrystalline titania optical thin films, Eur. Polym. J. 45 (2009) 2749–2759.
[4] S. Srisuwan, S. Thongyai, P. Praserthdam, Synthesis and characterization of low-dielectric photosensitive polyimide/silica hybrid materials, J. Appl. Polym. Sci. 117 (2010) 2422–2427.
[5] X. Duthie, S. Kentish, C. Powell, K. Nagai, G. Qiao, G. Stevens, Operating temperature effects on the plasticization of polyimide gas separation membranes, J. Membr. Sci. 294 (2007) 40–49.
[6] S. Miyata, S. Sato, K. Nagai, T. Nakagawa, K. Kudo, Relationship between gas transport properties and fractional free volume determined from dielectric constant in polyimide films containing the hexafluoroisopropylidene group, J. Appl. Polym. Sci. 107 (2008) 3933–3944.
[7] S. Kanehashi, T. Nakagawa, K. Nagai, X. Duthie, S. Kentish, G. Stevens, Effects of carbon dioxide-induced plasticization on the gas transport properties of glassy polyimide membranes, J. Membr. Sci. 298 (2007) 147–155.
[8] S. Sato, M. Suzuki, S. Kanehashi, K. Nagai, Permeability, diffusivity, and solubility of benzene vapor and water vapor in high free volume silicon- or fluorine-containing polymer membranes, J. Membr. Sci. 360 (2010) 352–362.
[9] S. Matsui, T. Nakagawa, Effect of ultraviolet light irradiation on gas permeability in polyimide membranes. II. Irradiation of membranes with high-pressure mercury lamp, J. Appl. Polym. Sci. 67 (1998) 49–60.
[10] Y. Liu, C. Pan, M. Ding, J. Xu, Effect of crosslinking distribution on gas permeability and permselectivity of crosslinked polyimides, Eur. Polym. J. 35 (1999) 1739–1741.
[11] H. Kita, T. Inada, K. Tanaka, K. Okamoto, Effect of photo-cross-linking on permeability and permselectivity of gases through benzophenone-containing polyimide, J. Membr. Sci. 87 (1994) 139–147.
[12] S. Matsui, T. Ishiguro, A. Higuchi, T. Nakagawa, Effect of ultraviolet light irradiation on gas permeability in polyimide membranes. 1. Irradiation with low pressure mercury lamp on photosensitive and nonphotosensitive membranes, J. Polym. Sci., Part B: Polym. Phys. 35 (1997) 2259–2269.
[13] S. Matsui, H. Sato, T. Nakagawa, Effects of low molecular weight photosensitizer and UV irradiation on gas permeability and selectivity of polyimide membrane, J. Membr. Sci. 141 (1998) 31–43.
[14] J.H. Kim, W.J. Koros, D.R. Paul, Effects of CO_2 exposure and physical aging on the gas permeability of thin 6FDA-based polyimide membranes – Part 2. with crosslinking, J. Membr. Sci. 282 (2006) 32–43.
[15] C.T. Wright, D.R. Paul, Gas sorption and transport in UV-irradiated poly(2,6-dimethyl-1,4-phenylene oxide) films, J. Appl. Polym. Sci. 67 (1998) 875–883.
[16] Y. Liu, M.X. Ding, J.P. Xu, Gas permeabilities and permselectivity of photochemically cross-linked polyimides, J. Appl. Polym. Sci. 58 (1995) 485–489.
[17] I.K. Meier, M. Langsam, H.C. Klotz, Selectivity enhancement via photooxidative surface modification of polyimide air separation membranes, J. Membr. Sci. 94 (1994) 195–212.
[18] I.K. Meier, M. Langsam, Photochemically induced oxidative surface modification of polyimide films, J. Polym. Sci., Part A: Polym. Chem. 31 (1993) 83–89.
[19] T. Komatsuka, A. Kusakabe, K. Nagai, Characterization and gas transport properties of poly(lactic acid) blend membranes, Desalination 234 (2008) 212–220.
[20] T. Komatsuka, K. Nagai, Temperature dependence on gas permeability and permselectivity of poly(lactic acid) blend membranes, Polym. J. 41 (2009) 455–458.
[21] L.M. Robeson, The upper bound revisited, J. Membr. Sci. 320 (2008) 390–400.